



HAL
open science

Higher temperature variability reduces temperature sensitivity of vegetation growth in Northern Hemisphere

Xiuchen Wu, Hongyan Liu, Xiaoyan Li, Shilong Piao, Philippe Ciais, Weichao Guo, Yi Yin, Ben Poulter, Changhui Peng, Nicolas Viovy, et al.

► To cite this version:

Xiuchen Wu, Hongyan Liu, Xiaoyan Li, Shilong Piao, Philippe Ciais, et al.. Higher temperature variability reduces temperature sensitivity of vegetation growth in Northern Hemisphere. *Geophysical Research Letters*, 2017, 44 (12), pp.6173-6181. 10.1002/2017GL073285 . hal-02903704

HAL Id: hal-02903704

<https://hal.science/hal-02903704>

Submitted on 6 May 2021

HAL is a multi-disciplinary open access archive for the deposit and dissemination of scientific research documents, whether they are published or not. The documents may come from teaching and research institutions in France or abroad, or from public or private research centers.

L'archive ouverte pluridisciplinaire **HAL**, est destinée au dépôt et à la diffusion de documents scientifiques de niveau recherche, publiés ou non, émanant des établissements d'enseignement et de recherche français ou étrangers, des laboratoires publics ou privés.



Distributed under a Creative Commons Attribution 4.0 International License



RESEARCH LETTER

10.1002/2017GL073285

Key Points:

- It shows consistent decrease in temperature sensitivity of vegetation growth by temperature variability for all vegetation types
- Larger decrease in temperature sensitivity of vegetation growth by temperature variability is found in forest and shrub in dry regions
- Drier condition adds further decrease in temperature sensitivity of vegetation growth by temperature variability for forest and shrub in dry regions

Supporting Information:

- Supporting Information S1

Correspondence to:

X. Li and X. Wu,
xyli@bnu.edu.cn;
xiuchen.wu@bnu.edu.cn

Citation:

Wu, X., et al. (2017), Higher temperature variability reduces temperature sensitivity of vegetation growth in Northern Hemisphere, *Geophys. Res. Lett.*, 44, 6173–6181, doi:10.1002/2017GL073285.

Received 11 MAR 2017

Accepted 7 JUN 2017

Accepted article online 9 JUN 2017

Published online 28 JUN 2017

©2017. American Geophysical Union.
All Rights Reserved.

Higher temperature variability reduces temperature sensitivity of vegetation growth in Northern Hemisphere

Xiuchen Wu^{1,2} , Hongyan Liu³ , Xiaoyan Li^{1,2} , Shilong Piao^{3,4} , Philippe Ciais⁵, Weichao Guo³, Yi Yin⁵ , Ben Poulter⁶ , Changhui Peng⁷, Nicolas Viovy⁵, Nicolas Vuichard⁵, Pei Wang^{1,2}, and Yongmei Huang^{1,2}

¹State Key Laboratory of Earth Surface Processes and Resource Ecology, Beijing Normal University, Beijing, China, ²School of Natural Resources, Faculty of Geographical Science, Beijing Normal University, Beijing, China, ³College of Urban and Environmental Science, Peking University, Beijing, China, ⁴Key Laboratory of Alpine Ecology and Biodiversity, Institute of Tibetan Plateau Research, Chinese Academy of Sciences, Beijing, China, ⁵CEA-CNRS-UVSQ, UMR8212-Laboratoire des Sciences du Climat et de l'Environnement, Gif-Sur-Yvette, France, ⁶Department of Ecology and Institute on Ecosystems, Montana State University, Bozeman, Montana, USA, ⁷Institute of Environment Sciences, University of Quebec at Montreal, Montreal, Quebec, Canada

Abstract Interannual air temperature variability has changed over some regions in Northern Hemisphere (NH), accompanying with climate warming. However, whether and to what extent it regulates the interannual sensitivity of vegetation growth to temperature variability (i.e., interannual temperature sensitivity)—one central issue in understanding and predicting the responses of vegetation growth to changing climate—still remains poorly quantified and understood. Here we quantify the relationships between the interannual temperature sensitivity of mean growing-season (April–October) normalized difference vegetation index (NDVI) and ecosystem model simulations of gross primary productivity (GPP), and variability in mean growing-season temperature for forest, shrub, and grass over NH. We find that higher interannual variability in mean growing-season temperature leads to consistent decrease in interannual temperature sensitivity of mean growing-season NDVI among all vegetation types but not in model simulations of GPP. Drier condition associates with $\sim 130 \pm 150\%$ further decrease in interannual temperature sensitivity of mean growing-season NDVI by temperature variability in forest and shrub. These results illustrate that varying temperature variability can significantly regulate the interannual temperature sensitivity of vegetation growth over NH, interacted with drought variability and nonlinear responses of photosynthesis to temperature. Our findings call for an improved characterization of the nonlinear effects of temperature variability on vegetation growth within global ecosystem models.

1. Introduction

Vegetation growth in temperate (30°–50°N) and boreal (>50°N) Northern Hemisphere (NH) is tightly coupled with interannual variability of the mean growing-season temperature (IAV_{GT}) [Nemani et al., 2003; Piao et al., 2014]. This biological response has been attributed to how temperature variability limits primarily carbon-cycle processes (photosynthesis and respiration), phenology, and hydrothermal conditions (e.g., evapotranspiration, snow cover, and melting dynamics) [Barichivich et al., 2013; Heimann and Reichstein, 2008; Nemani et al., 2003; Piao et al., 2007; Wang et al., 2011]. At regional scales, the correlation between vegetation growth and interannual variability of temperature varies spatially and temporally within the NH [Barichivich et al., 2013; Piao et al., 2011; Wu et al., 2016]. In particular, recent studies using both satellite observations and ground-truth tree growth measurements documented a weakening correlation between terrestrial vegetation growth and IAV_{GT} in many parts of NH, i.e., the “divergence problem” [Buermann et al., 2014; D’Arrigo et al., 2008; Piao et al., 2014]. Several hypotheses have been proposed to explain the divergence problem, including increased drought stress and nonlinear temperature responses [D’Arrigo et al., 2008; Piao et al., 2014]. Besides, terrestrial vegetation growth is particularly susceptible to short-term, episodic climate fluctuations, such as recurring heat waves and mega-droughts [Allen et al., 2010; Breshears et al., 2005; Ciais et al., 2005; Haverd et al., 2016; Poulter et al., 2014; Reichstein et al., 2007]. Increasing evidence shows that terrestrial vegetation growth has responded more to changing temperature variability than to changing mean temperature [Ciais et al., 2005; Reichstein et al., 2013].

Accompanying with rapidly changing climate, driven by both external forcings and internal decadal and/or interannual oscillations of climate systems, the temperature variability could also change spatiotemporally. In fact, marked changes (increase or decrease) in temperature variability have already been documented in some regions, as exemplified in Europe and East Asia [Ito et al., 2013; Schar et al., 2004], particularly over temperate NH [Marotzke and Forster, 2015; Sippel et al., 2015]. However, whether and to what extent temperature variability regulates the interannual temperature sensitivity of vegetation growth for diverse vegetation types over NH still remains poorly quantified and understood.

The lack of an integrative analysis into both the direction and magnitude of the interannual temperature sensitivity of vegetation growth regulated by temperature variability across diverse vegetation types and hydrothermal conditions limits accurate predictions of how will northern terrestrial ecosystems respond to a warmer and more extreme climate [Bahn et al., 2014; Barriopedro et al., 2011; Field, 2012; IPCC, 2013]. Here we hypothesize that temperature variability markedly but differently regulates the interannual temperature sensitivity of vegetation growth across diverse vegetation types over NH.

In this study, we aim to quantify these patterns by analyzing observed relationships between the interannual temperature sensitivity of vegetation growth and IAV_{GT} during 1982–2012, using the latest satellite-derived normalized difference vegetation index (NDVI) from the GIMMS (Global Inventory Modeling and Mapping Studies) group (i.e., GIMMS NDVI3g), global ecosystem model simulations of gross primary productivity (GPP), and gridded climate data for forest, shrub, and grass in seven climate zones over NH.

2. Methods

2.1. Vegetation and Climate Data Sets

2.1.1. GIMMS NDVI3g Data Set

The biweekly advanced very high resolution radiometer NDVI data during 1982–2012 were obtained from the GIMMS group (i.e., GIMMS NDVI3g), with a spatial resolution of 0.083° . They were aggregated into a spatial resolution of 0.5° to fit gridded climate data (see below). The GIMMS NDVI3g data have been extensively corrected for contaminations from cloud cover, aerosols, sensor degradation, navigational drift, solar zenith angle, viewing angle effects due to satellite drift, and volcanic aerosols [Tucker et al., 2005]. GIMMS NDVI3g data have been widely used in studies of monitoring vegetation activity [Buermann et al., 2014; Piao et al., 2014], phenology [Piao et al., 2015], and productivity [Guay et al., 2014].

2.1.2. Climate Data Sets

Gridded monthly air temperature and precipitation data with spatial resolution of 0.5° during 1982–2012 were obtained from the Climate Research Unit (CRU) TS 3.23 data sets, compiled by the Climate Research Unit of University of East Anglia [Harris et al., 2014]. The downward shortwave solar radiation data with spatial resolution of 0.5° were obtained from the CRU-National Centers for Environmental Prediction (NCEP) product (<http://dods.extra.cea.fr/store/p529viov/cruncep/>). The gridded CRU-NCEP data are a harmonized product combining CRU TS 3.23 and NCEP-NCAR reanalysis, providing 6-hourly meteorological forcing for global land surface model simulations [Mao et al., 2012; Sitch et al., 2008]. A global gridded monthly self-calibrated Palmer Drought Severity Index (scPDSI) data set at a spatial resolution of 0.5° with the potential evapotranspiration estimated using the Penman-Monteith equation is calculated based on the updated climate data of CRU TS 3.22 and obtained from the KNMI Climate Explorer (<http://climexp.knmi.nl/select.cgi?id=someone@some-where&field=scpdsi>). This data set has several methodological improvements that allow a better spatial-temporal quantification of drought at northern latitudes [Schrier et al., 2013; Sheffield et al., 2012; van der Schrier et al., 2006]. A global aridity index database with a spatial resolution of 30 arcsec (<http://www.cgiar-csi.org/data/global-aridity-and-pet-database>) was used to estimate the aridity conditions within different climate zones.

2.2. Global Ecosystem Models

Two process-based global ecosystem models, LPJ (Lund-Potsdam-Jena) and ORCHIDEE (ORganizing Carbon and Hydrology In Dynamic Ecosystem), were used in this study to simulate the terrestrial GPP in temperate and boreal NH over the period of 1980–2010. All simulations followed the protocol described in the TRENDY project (Trends in Net Land Atmosphere Carbon Exchanges) (http://dgvn.ceh.ac.uk/system/files/Trendy_protocol%20_Nov2011_0.pdf). All models used in this study prescribed static vegetation maps. Each model was run from its preindustrial equilibrium (assumed here at the beginning of the 1900s) to

2010. Each model was forced by both observed historic climate changes and rising CO₂ concentrations, as described in the S2 scenario in TRENDY.

2.3. Statistical Analyses

Ridge regression was applied to calculate the interannual sensitivity (i.e., the regression coefficients) of vegetation growth, from perspectives of both NDVI and simulated GPP, to variability of mean growing-season temperature, scPDSI, and solar radiation during 1982–2012 in temperate and boreal NH. Mean growing-season NDVI and summed growing-season GPP are used in this study as effective indicators of vegetation growth. Growing season for vegetation is consistently defined here as from April to October in temperate and boreal NH [Piao *et al.*, 2014]. All variables are linearly detrended prior to the ridge regression. Ridge regression is verified as an effective method that can reduce the collinearity between independent variables and get a robust estimation of the regression coefficients [Hoerl and Kennard, 1970].

Positive and negative interannual sensitivity of vegetation growth to climate variability are separately identified by ridge regression for each kind of vegetation types in each of the seven climate zones (see below). Exponential quantile regression is then applied to investigate the relationships between the interannual climate sensitivity of vegetation growth and the climate variability for forest, shrub, and grass in each climate zone for the two response modes. The fitted parameter β of interannual variability of climate $|IAV_i|$, in the exponential quantile regression (equation (1)) for the relationships between the interannual climate sensitivity of vegetation growth (γ_i) and interannual variability of climate variable are then used to assess the magnitude of decrease/increase in interannual climate sensitivity of vegetation growth by climate variability. A negative β implies decrease in interannual climate sensitivity of vegetation growth.

$$\gamma_i = \alpha \times \exp^{\beta |IAV_i|} \quad (1)$$

Seven major climate zones are reclassified based on the Köppen-Geiger climate classification [Kottek *et al.*, 2006], including arid, temperate dry, temperate humid, cold summer dry, cold winter dry, cold humid, and tundra regions (Table S1 and Figure S1 in the supporting information). In our study, grids with elevation higher than the 90th percentile of elevation distribution in each of climate zones are discarded from our final analyses of the relationship between the interannual climate sensitivity of vegetation growth and climate variability, based on the GTOPO30 data set (<https://lta.cr.usgs.gov/GTOPO30>).

3. Results

3.1. Interannual Sensitivity of Vegetation Growth to Mean Growing-Season Climate

We first investigate the spatial patterns in the interannual sensitivity of vegetation growth to mean growing-season (April–October) climate in NH. We observe generally negative and positive sensitivity of mean growing-season NDVI (NDVI_{G5}) and GPP (GPP_{G5}) to mean growing-season temperature in temperate (30°N–50°N) and boreal (>50°N) NH, respectively, despite great spatial variations and potentially confounding effects of other factors, e.g., land use and disturbances (Figures 1a and S2–S4). There is a predominantly (~75%) negative sensitivity of NDVI_{G5} to mean growing-season temperature in arid climate zone, with statistical significance ($p < 0.05$) in ~26% of this region (Table S1 and S5). In contrast, we observe a predominantly positive sensitivity of NDVI_{G5} to mean growing-season temperature in four cold climate zones (71%–93%), including cold summer dry, cold winter dry, cold humid, and tundra climate zones, with statistically significant sensitivity in 26%–50% of these regions. The sensitivity of NDVI_{G5} to mean growing-season temperature in temperate arid and temperate humid climate zones shows large spatial variations, attributed primarily to spatial difference in hydrological conditions, as well as vegetation types and soil properties, which partly confound the generalization of sensitivity of NDVI_{G5} to mean growing-season temperature across the entire biogeographic region (Figures 1a and S2) [see also Piao *et al.*, 2014, Figure 2; Barichivich *et al.*, 2013, Figure 3].

In contrast, we observe a dipole pattern in the interannual sensitivity of vegetation growth to mean growing-season water availability, using both the self-calibrating Palmer Drought Severity Index (scPDSI) and Standardized Precipitation-Evapotranspiration Index (SPEI) as proxies. Compared to mean growing-season temperature (Figures 1b and S2 and S6), positive sensitivity of NDVI_{G5} to mean growing-season scPDSI and SPEI are observed in temperate NH, mainly in Central America, the Mediterranean region, and mid-latitude Eurasia (Figures 1b and S2 and S6). However, the spatial patterns in sensitivity of NDVI_{G5} to mean

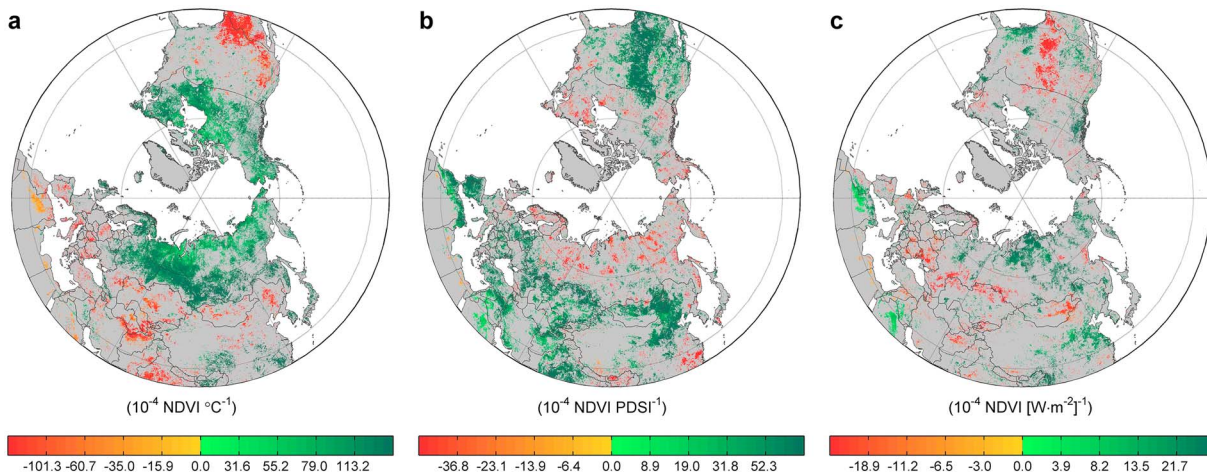


Figure 1. Spatial patterns in the interannual sensitivity of mean growing-season (April–October) normalized difference vegetation index ($NDVI_{GS}$) to mean growing-season climate. (a–c) The interannual sensitivity of $NDVI_{GS}$ to mean growing-season temperature, mean growing-season scPDSI, and mean growing-season short-wave solar radiation is shown. The interannual sensitivity of $NDVI_{GS}$ to mean growing-season climate is calculated by the coefficients of ridge regression (in detail see section 2). Data shown here are statistically significant ($p < 0.05$).

growing-season scPDSI and SPEI are ambiguous in boreal NH, with significantly negative one observed in only 5.1%–8.8% of boreal NH (Figures S6 and S7). Consistent spatial patterns are also observed between the drought indices and the simulated GPP of two global ecosystem models, LPJ and ORCHIDEE, but a larger area with positive sensitivity of GPP_{GS} to mean growing-season scPDSI and SPEI in boreal NH (Figures S3 and S4). The difference between the sensitivity of GPP_{GS} simulation by global ecosystem models and $NDVI_{GS}$ to drought indices in boreal NH has also been reported in recent studies [e.g., Piao *et al.*, 2014]. By contrast, the sensitivity of $NDVI_{GS}$ to mean growing-season short-wave solar radiation shows great spatial heterogeneity over temperate and boreal NH (Figure 1c). Regions showing negative relationship between $NDVI_{GS}$ and short-wave solar radiation are generally concordant to that for temperature.

3.2. Decrease in the Interannual Temperature Sensitivity of Vegetation Growth by IAV_{GT}

We then quantify the direction and the magnitude in the interannual sensitivity of vegetation growth to temperature (hereafter as interannual temperature sensitivity) by IAV_{GT} across the seven climate zones for forest, shrub and grass, using adaptive exponential regressions at the 50th quantile (see section 2). We reveal a consistent decrease in interannual temperature sensitivity of $NDVI_{GS}$ by higher IAV_{GT} (using space-for-time substitution), evaluated by the absolute value of the coefficient of variation of mean growing-season temperature ($|CV_{GT}|$), in both positive and negative modes of interannual temperature sensitivity of $NDVI_{GS}$ for forest, shrub, and grass across seven climate zones (Figure 2). The relationship between interannual temperature sensitivity of $NDVI_{GS}$ (γ_{GT}^{NDVI}) and $|CV_{GT}|$ for forest, shrub, and grass across diverse climate zones is characterized by equation of $\gamma_{GT}^{NDVI} = \alpha \times \exp(\beta_{GT} |CV_{GT}|)$. A negative β_{GT} implies decrease in γ_{GT}^{NDVI} by higher $|CV_{GT}|$ (Figure 2). The values of β_{GT} are then used to quantify the magnitude of decrease in γ_{GT}^{NDVI} by $|CV_{GT}|$ (see section 2 for more details). The β_{GT} shows large variations across different climate zones and vegetation types (Table S2 and Figure 2). For the deep-rooted forest and shrub, more negative β_{GT} is observed in arid, temperate arid, and temperate humid regions for both positive and negative modes of γ_{GT}^{NDVI} (Table S2 and Figure 2). Within each climate zone, more negative β_{GT} is consistently observed in drier regions (with multiyear mean scPDSI < 25th percentile of regional distribution of multiyear mean scPDSI) than in wetter (with multiyear mean scPDSI > 75th percentile of regional distribution of multiyear mean scPDSI) regions for all three vegetation types (Figure S8). The β_{GT} across different climate zones does not show strong relationships with either regional mean water conditions (represented by aridity index) (Figure 3) or linear trends in mean growing-season scPDSI during 1982–2012 in both positive and negative modes of γ_{GT}^{NDVI} for three vegetation types (Figures S9).

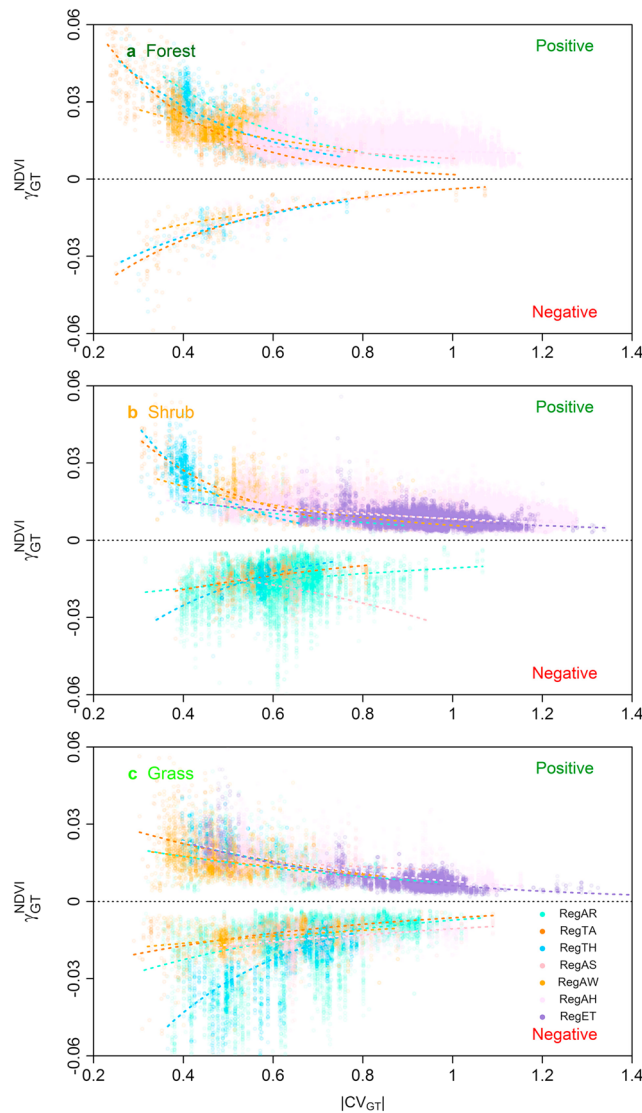


Figure 2. Relationships between the interannual sensitivity of mean growing-season (April–October) normalized difference vegetation index (γ_{GS}^{NDVI}) to mean growing-season temperature (γ_{GT}^{NDVI}) and the interannual variability of mean growing-season temperature in seven major climate zones for (a) forest, (b) shrub, and (c) grass. The interannual variability of mean growing-season temperature is represented by the absolute coefficient of variation of mean growing-season temperature (i.e., $|CV_{GT}|$). In this study, seven major climate zones are reclassified based on the Köppen-Geiger climate classification, including arid (RegAR), temperate arid (RegTA), temperate humid (RegTH), cold summer dry (RegAS), cold winter dry (RegAW), cold humid (RegAH), and tundra (RegET) regions. We divided γ_{GT}^{NDVI} into positive and negative response modes for each kind of vegetation types across each climate zone. The fitted lines in this figure are the significantly exponential regression lines at 50th quantile. Data shown here are high-elevation filtered to avoid specific feature regarding the vegetation responses to climate in high altitudinal zones (in detail see section 2).

By contrast, we did not observe consistent decrease in interannual temperature sensitivity of GPP_{GS} (γ_{GT}^{GPP}) by higher $|CV_{GT}|$ in the simulated GPP from either LPJ or ORCHIDEE for different vegetation types (Figures S10 and S11). The observed decrease in γ_{GT}^{NDVI} by higher $|CV_{GT}|$ across different climate zones for all three kinds of vegetation types cannot be explained by the nonunified relationships between γ_{GT}^{NDVI} and mean growing-season NDVI in different climate zones (Figure S12).

Moreover, we observe a consistent decrease in $|CV_{GT}|$ for forest areas across different climate zones during 1982–2012, with 59%–76% of those areas showing decreasing $|CV_{GT}|$ (Figure S13). Decreasing $|CV_{GT}|$ is also observed in arid and temperate climate zones for shrub (58%–65%) and grass (59%–77%) (Figure S13). However, $|CV_{GT}|$ is not consistently decreasing in cold climate zones of NH for shrub and grass during 1982–2012 (Figure S13).

4. Discussion

Shifts in temperature variability have been reported to be potentially more important than changes in mean temperature for terrestrial ecosystems functioning [Screen, 2014]. Therefore, quantification of effects of temperature variability on the regulations of interannual temperature sensitivity of vegetation growth is a critical, but overlooked, prerequisite for accurately predicting stability/resilience of northern terrestrial ecosystems in response to a warmer and more extreme climate [Jump and Peñuelas, 2005; Watson et al., 2013]. Here we statistically report a consistent decrease in interannual temperature sensitivity of vegetation growth by higher interannual variability of mean growing-season temperature for all three kinds of vegetation types across seven climate zones in satellite-derived

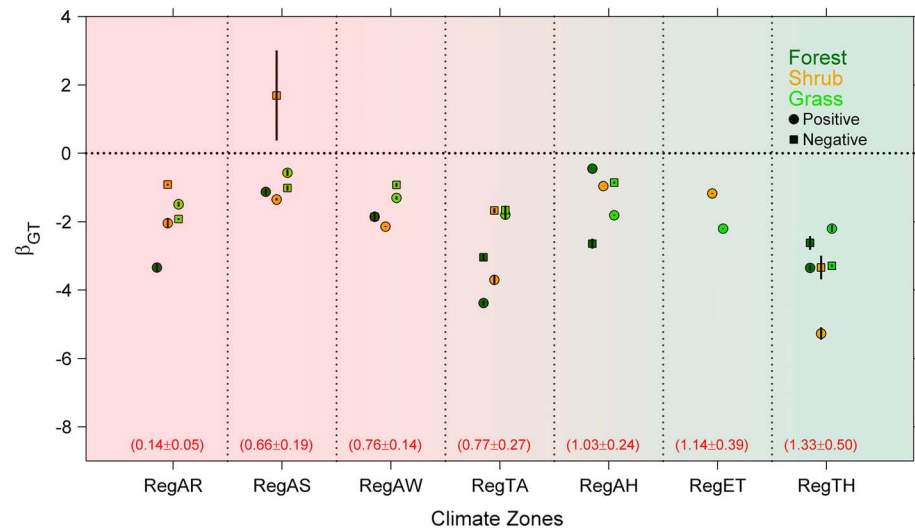


Figure 3. Distribution of the fitted parameters of the interannual variability of mean growing-season temperature (CV_{GT}) in the relationships between interannual sensitivity of mean growing-season NDVI to GT (γ_{GT}^{NDVI}) and interannual variability of GT (i.e., β_{GT} in $\gamma_{GT}^{NDVI} = \alpha \times \exp(\beta_{GT} |CV_{GT}|)$) along with the aridity index in different climate zones for forest, shrub, and grass. In this study, seven major climate zones are reclassified based on the Köppen-Geiger climate classification, including arid (RegAR), temperate arid (RegTA), temperate humid (RegTH), cold summer dry (RegAS), cold winter dry (RegAW), cold humid (RegAH), and tundra (RegET) regions. We divided γ_{GT}^{NDVI} into positive and negative response modes for each kind of vegetation types in each climate zone, respectively. The bars represent the confidence intervals at 95% level. The regional mean aridity index for different climate zones is shown in mean \pm standard deviations (red numbers in parentheses). The darker red and green background colors of this figure indicate much drier and wetter climate conditions.

measurements. The underlying mechanisms cannot be directly elucidated from our statistical analyses and are hypothesized to be different in water-limited and thermal-limited climate zones.

In water-limited climate zones (mostly located in temperate NH), temperature variability affects water availability and consequently eco-physiological processes (e.g., canopy conductance) within soil-vegetation-atmosphere systems [Barichivich *et al.*, 2014; Ma *et al.*, 2012], and thus regulates the interannual temperature sensitivity of vegetation growth. Specifically, higher interannual variability of mean growing-season temperature can potentially cause a higher variations in water conditions in water-limited climate zones (Figure S1), owing to its effects on evaporative demands and low water conservation capacity, particularly in semiarid conditions [Huang *et al.*, 2012]. Under a more variable drought stress, plants are expected to have better hydrological drought tolerance/avoidance acclimation, depending also on trait-based eco-hydrological strategies (see below), and thus exhibit a lower interannual temperature sensitivity. The negative relationships between interannual temperature sensitivity of $NDVI_{GS}$ and variations in multiyear mean growing-season $sPDSI$ for all vegetation types in arid and temperate arid climate zones are consistent with a lower interannual temperature sensitivity of vegetation growth in response to higher variations of drought stress (Figure S14). A recent study reported that climate warming-induced increasing drought stress causes a temporally weakening coupling between vegetation growth and interannual variability of growing-season temperature in water-limited temperate NH [Piao *et al.*, 2014]. We further found that more drought stress coincides with a larger decrease in interannual temperature sensitivity of $NDVI_{GS}$ by higher variations in growing-season temperature within each of these water-limited climate zones for all three vegetation types (Figure S8). Tree ring measurements also reveal that increasing drought stress contributes largely to the observed decreasing temperature sensitivity of tree growth to temperature variability in recent decades (the “divergence problem”) in extratropical NH [D’Arrigo *et al.*, 2008; Wu *et al.*, 2013]. In thermal-limited climate zones (primarily located in boreal NH), the consistent decrease in interannual temperature sensitivity of vegetation growth by higher variations in growing-season temperature is not attributed to asynchronous effects of temperature variability on water conditions across different climate zones (Figure S1). Nonetheless, the explicit mechanisms remain unclear.

Beside the consistent decrease in interannual temperature sensitivity of vegetation growth, the difference in the magnitudes across different climate zones cannot be explained by differences in either regional mean

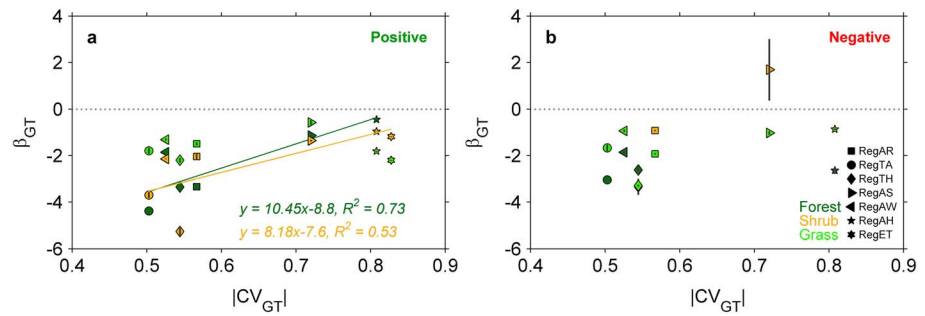


Figure 4. Relationships between the fitted parameters of the interannual variability of mean growing-season temperature ($|CV_{GT}|$) in the relationships between interannual sensitivity of mean growing-season NDVI to GT (γ_{GT}^{NDVI}) and interannual variability of GT (i.e., β_{GT} in $\gamma_{GT}^{NDVI} = \alpha \times \exp(\beta_{GT} |CV_{GT}|)$) and $|CV_{GT}|$ for different vegetation types across climate zones. In this study, seven major climate zones are reclassified based on the Köppen-Geiger climate classification, including arid (RegAR), temperate arid (RegTA), temperate humid (RegTH), cold summer dry (RegAS), cold winter dry (RegAW), cold humid (RegAH), and tundra (RegET) regions. We divided γ_{GT}^{NDVI} into positive and negative response modes for each kind of vegetation types in each climate zone, respectively. The solid lines indicate significant linear fits between β_{GT} and $|CV_{GT}|$.

water conditions (represented by the aridity index) (Figure 3) or mean growing-season scPDSI during 1982–2012 for two modes in interannual temperature sensitivity of $NDVI_{GS}$ for any vegetation type (Figure S9). Here we propose two possible mechanisms to partly explain the differences in the decrease magnitudes in interannual temperature sensitivity of $NDVI_{GS}$ by variations in growing-season temperature. The first one is the difference in eco-hydrological traits among different vegetation types. Larger decrease in interannual temperature sensitivity of $NDVI_{GS}$ is observed mainly in deep-rooted forest and shrub in arid and temperate regions (Figure 4). Deep-rooted vegetation was previously thought to be more resilient and less sensitive to variations of climate in water-limited regions than shallow-rooted vegetation [Sala *et al.*, 2015], attributed to the deep root system and adaptive water use strategy [Asbjornsen *et al.*, 2008; Eggemeyer *et al.*, 2009]. However, the hydraulic corollary to Darcy's law, a core principle of vascular plant physiology, predicts that taller plants are becoming more vulnerable to temperature variability-mediated changes in vapor pressure deficits and their consequent effects on canopy water conductance and vegetation growth [McDowell and Allen, 2015], particularly under enhanced warming in semiarid regions and more extreme climate [Huang *et al.*, 2012; Reichstein *et al.*, 2013] (Figure 4). There is increasing evidence that taller plants growing in water-limited climate zones have suffered increased mortality during the past decades [McDowell and Allen, 2015]. To survive under a more variable climate in these water-limited regions, taller plants have to quickly modify the soil-to-leaf water potential difference and/or decrease the leaf area (e.g., tree crown dieback) [McDowell and Allen, 2015], depending also on two contrasting trait-based water management strategies. From an evolutionary perspective, environmental variability represents a selection pressure that results in physiological plasticity for taller plants to quickly cope with temperature mediated changes in drought stress. This can be partly explained by the observed more negative fitting coefficient β_{GT} in equation $\gamma_{GT}^{NDVI} = \alpha \times \exp(\beta_{GT} |CV_{GT}|)$ for forest and shrub in water-limited regions (Figure 4).

The second possible mechanism is the threshold-based nonlinear temperature responses of vegetation growth. In boreal NH, possible differences in threshold-based nonlinear temperature responses of vegetation growth across different climate zones and vegetation types can contribute to the observed difference in decrease magnitudes of interannual temperature sensitivity of vegetation growth by interannual variability of growing-season temperature [Piao *et al.*, 2014]. Undoubtedly, the difference in vegetation structures, historical disturbance regimes, and edaphic conditions can also affect the decrease magnitudes of the interannual temperature sensitivity of vegetation growth to temperature variability within and between climate zones and vegetation types. However, we do not take these factors into account in our analyses due to lack of sufficient records.

Finally, caution should be exercised in predictions of the stability of terrestrial vegetation growth in a warmer and more extreme climate, since the current global ecosystem modeling frameworks cannot reproduce the consistent decrease in interannual temperature sensitivity of vegetation growth by temperature variability observed from remote sensing measurements. Further, the intrinsic linkage between changing interannual

temperature sensitivity and its effects on regional vegetation growth interacted with other factors still remains poorly understood, as exemplified with arctic greening while following a decrease in interannual temperature sensitivity of vegetation growth in the same region [Macias-Fauria et al., 2012; Forbes et al., 2010]. Comprehensive studies are urgently needed to identify the mechanisms underlying the regulations of temperature variability on interannual temperature sensitivity and their effects on regional vegetation growth, combining long-term and large-scale data streams from multiple perspectives, including remote sensing observations, tree ring measurements, and other paleo-proxies.

5. Conclusions

Our analyses clearly reveal a consistent decrease in interannual temperature sensitivity of vegetation growth by temperature variability in forest, shrub, and grass across seven climate zones in NH in satellite measurements of vegetation indices. Larger decrease is observed in taller forest and shrub in water-limited arid and temperate climate zones. These findings support our hypothesis that temperature variability markedly but differently regulates the interannual temperature sensitivity of vegetation growth over NH. The differences in the decrease magnitudes across different climate zones and vegetation types are attributed to interactions of different mechanisms, including difference in eco-hydrological traits, difference in nonlinear temperature responses and other confounding factors (e.g., historical disturbance regimes and land cover changes). Our analyses provide insights into the future trajectory of northern ecosystems in response to a shifting climate regime characterized by changes in both mean climate state and potential climate variability/extreme events. Our findings call for an improved characterization of the nonlinear effects of temperature variations on vegetation growth to better predict northern ecosystem stability in response to a warmer and more extreme world. Finally, to accurately predict future ecosystem dynamics, the terrestrial carbon cycle, and its climate feedback in the Northern Hemisphere, deeper understanding of the mechanisms underlying the consistent decrease in interannual temperature sensitivity of vegetation growth by temperature variability across different vegetation types and climate zones is urgently needed, particularly using improved ecosystem models.

Acknowledgments

We thank all investigators in the TRENDY project. X.L. was supported by the National Natural Science Foundation of China (grant 41390462), the PCSIRT (grant IRT_15R06), and projects from the State Key Laboratory of Earth Surface Processes and Resource Ecology. X.W. was supported by the National Natural Science Foundation of China (grant 41571038) and projects from the State Key Laboratory of Earth Surface Processes and Resource Ecology (grant 2017-ZY-06). H.L. was financially supported by the National Natural Science Foundation of China (grants 41325002 and 41530747). All remote sensing and climate data used in this study are public. The GIMMS NDVI3g data can be obtained from <https://nex.nasa.gov/nex/projects/1349/>; the CRU TS 3.23 data are downloaded from https://crudata.uea.ac.uk/cru/data/hrgr/cru_ts_3.23/. Gross primary production simulations from models involved in TRENDY project can be obtained from <http://dgvn.ceh.ac.uk/node/9/index.html>. All coauthors declare that there is no conflict of interests.

References

- Allen, C. D., A. K. Macalady, H. Chenchouni, D. Bachelet, N. McDowell, M. Vennetier, T. Kitzberger, A. Rigling, D. D. Breshears, and E. T. Hogg (2010), A global overview of drought and heat-induced tree mortality reveals emerging climate change risks for forests, *For. Ecol. Manag.*, *259*(4), 660–684.
- Asbjornsen, H., G. Shepherd, M. Helmers, and G. Mora (2008), Seasonal patterns in depth of water uptake under contrasting annual and perennial systems in the Corn Belt region of the Midwestern US, *Plant Soil*, *308*(1–2), 69–92.
- Bahn, M., M. Reichstein, J. S. Dukes, M. D. Smith, and N. G. McDowell (2014), Climate–biosphere interactions in a more extreme world, *New Phytol.*, *202*(2), 356–359.
- Barichivich, J., K. R. Briffa, R. B. Myneni, T. J. Osborn, T. M. Melvin, P. Ciais, S. Piao, and C. Tucker (2013), Large-scale variations in the vegetation growing season and annual cycle of atmospheric CO₂ at high northern latitudes from 1950 to 2011, *Glob. Chang. Biol.*, *19*(10), 3167–3183.
- Barichivich, J., K. Briffa, R. Myneni, G. Schrier, W. Dorigo, C. Tucker, T. Osborn, and T. Melvin (2014), Temperature and snow-mediated moisture controls of summer photosynthetic activity in northern terrestrial ecosystems between 1982 and 2011, *Remote Sens.*, *6*(2), 1390–1431.
- Barriopedro, D., E. M. Fischer, J. Luterbacher, R. M. Trigo, and R. García-Herrera (2011), The hot summer of 2010: Redrawing the temperature record map of Europe, *Science*, *332*(6026), 220–224.
- Breshears, D. D., N. S. Cobb, P. M. Rich, K. P. Price, C. D. Allen, R. G. Balice, W. H. Romme, J. H. Kastens, M. L. Floyd, and J. Belnap (2005), Regional vegetation die-off in response to global-change-type drought, *Proc. Natl. Acad. Sci. U.S.A.*, *102*(42), 15,144–15,148.
- Buermann, W., B. Parida, M. Jung, G. M. MacDonald, C. J. Tucker, and M. Reichstein (2014), Recent shift in Eurasian boreal forest greening response may be associated with warmer and drier summers, *Geophys. Res. Lett.*, *41*, 1995–2002, doi:10.1002/2014GL059450.
- Ciais, P., M. Reichstein, N. Viovy, A. Granier, J. Ogée, V. Allard, M. Aubinet, N. Buchmann, C. Bernhofer, and A. Carrara (2005), Europe-wide reduction in primary productivity caused by the heat and drought in 2003, *Nature*, *437*(7058), 529–533.
- D'Arrigo, R., R. Wilson, B. Liepert, and P. Cherubini (2008), On the 'divergence problem' in northern forests: A review of the tree-ring evidence and possible causes, *Glob. Planet. Chang.*, *60*(3), 289–305.
- Eggemeier, K. D., T. Awada, F. E. Harvey, D. A. Wedin, X. Zhou, and C. W. Zanner (2009), Seasonal changes in depth of water uptake for encroaching trees *Juniperus virginiana* and *Pinus ponderosa* and two dominant C4 grasses in a semiarid grassland, *Tree Physiol.*, *29*(2), 157–169.
- Field, C. B. (2012) *Managing the Risks of Extreme Events and Disasters to Advance Climate Change Adaptation: Special Report of the Intergovernmental Panel on Climate Change*, pp. 25–64, Cambridge Univ. Press, Cambridge.
- Forbes, B. C., M. Fauria, and P. Zetterberg (2010), Russian Arctic warming and 'greening' are closely tracked by tundra shrub willows, *Glob. Chang. Biol.*, *16*(5), 1542–1554.
- Guay, K. C., P. S. Beck, L. T. Berner, S. J. Goetz, A. Baccini, and W. Buermann (2014), Vegetation productivity patterns at high northern latitudes: A multi-sensor satellite data assessment, *Glob. Chang. Biol.*, *20*(10), 3147–3158.
- Harris, I., P. Jones, T. Osborn, and D. Lister (2014), Updated high-resolution grids of monthly climatic observations—the CRU TS3.10 dataset, *Int. J. Climatol.*, *34*(3), 623–642.

- Haverd, V., B. Smith, and C. Trustringer (2016), Dryland vegetation response to wet episode, not inherent shift in sensitivity to rainfall, behind Australia's role in 2011 global carbon sink anomaly, *Glob. Chang. Biol.*, *22*(7), 2315–2316.
- Heimann, M., and M. Reichstein (2008), Terrestrial ecosystem carbon dynamics and climate feedbacks, *Nature*, *451*(7176), 289–292.
- Hoerl, A. E., and R. W. Kennard (1970), Ridge regression: Biased estimation for nonorthogonal problems, *Technometrics*, *12*(1), 55–67.
- Huang, J. P., X. D. Guan, and F. Ji (2012), Enhanced cold-season warming in semi-arid regions, *Atmos. Chem. Phys.*, *12*(12), 5391–5398.
- IPCC (2013) *Climate Change 2013: The Physical Science Basis: Working Group I Contribution to the Fifth Assessment Report of the Intergovernmental Panel on Climate Change*, pp. 159–254, Cambridge Univ. Press, Cambridge.
- Ito, H., N. C. Johnson, and S. P. Xie (2013), Subseasonal and interannual temperature variability in relation to extreme temperature occurrence over East Asia, *J. Clim.*, *26*(22), 9026–9042.
- Jump, A. S., and J. Peñuelas (2005), Running to stand still: Adaptation and the response of plants to rapid climate change, *Ecol. Lett.*, *8*(9), 1010–1020.
- Kottek, M., J. Grieser, C. Beck, B. Rudolf, and F. Rubel (2006), World map of the Köppen-Geiger climate classification updated, *Meteorol. Z.*, *15*(3), 259–263.
- Ma, Z., C. Peng, Q. Zhu, H. Chen, G. Yu, W. Li, X. Zhou, W. Wang, and W. Zhang (2012), Regional drought-induced reduction in the biomass carbon sink of Canada's boreal forests, *Proc. Natl. Acad. Sci. U.S.A.*, *109*(7), 2423–2427.
- Macias-Fauria, M., B. C. Forbes, P. Zetterberg, and T. Kumpula (2012), Eurasian Arctic greening reveals teleconnections and the potential for structurally novel ecosystems, *Nat. Clim. Chang.*, *2*(8), 613–618.
- Mao, J., P. E. Thornton, X. Shi, M. Zhao, and W. M. Post (2012), Remote sensing evaluation of CLM4 GPP for the period 2000–09*, *J. Clim.*, *25*(15), 5327–5342.
- Marotzke, J., and P. M. Forster (2015), Forcing, feedback and internal variability in global temperature trends, *Nature*, *517*(7536), 565–570.
- McDowell, N. G., and C. D. Allen (2015), Darcy's law predicts widespread forest mortality under climate warming, *Nat. Clim. Chang.*, *5*(7), 669–672.
- Nemani, R. R., C. D. Keeling, H. Hashimoto, W. M. Jolly, S. C. Piper, C. J. Tucker, R. B. Myneni, and S. W. Running (2003), Climate-driven increases in global terrestrial net primary production from 1982 to 1999, *Science*, *300*(5625), 1560–1563.
- Piao, S., P. Friedlingstein, P. Ciais, N. Viovy, and J. Demarty (2007), Growing season extension and its impact on terrestrial carbon cycle in the Northern Hemisphere over the past 2 decades, *Global Biogeochem. Cycles*, *21*, GB3018, doi:10.1029/2006GB002888.
- Piao, S., X. Wang, P. Ciais, B. Zhu, T. A. O. Wang, and J. I. E. Liu (2011), Changes in satellite-derived vegetation growth trend in temperate and boreal Eurasia from 1982 to 2006, *Glob. Chang. Biol.*, *17*(10), 3228–3239.
- Piao, S., H. Nan, C. Huntingford, P. Ciais, P. Friedlingstein, S. Sitch, S. Peng, A. Ahlström, J. G. Canadell, and N. Cong (2014), Evidence for a weakening relationship between interannual temperature variability and northern vegetation activity, *Nat. Commun.*, *5*.
- Piao, S., J. Tan, A. Chen, Y. H. Fu, P. Ciais, Q. Liu, I. A. Janssens, S. Vicca, Z. Zeng, and S.-J. Jeong (2015), Leaf onset in the northern hemisphere triggered by daytime temperature, *Nat. Commun.*, *6*.
- Poulter, B., D. Frank, P. Ciais, R. B. Myneni, N. Andela, J. Bi, G. Broquet, J. G. Canadell, F. Chevallier, and Y. Y. Liu (2014), Contribution of semi-arid ecosystems to interannual variability of the global carbon cycle, *Nature*, *509*(7502), 600–603.
- Reichstein, M., P. Ciais, D. Papale, R. Valentini, S. Running, N. Viovy, W. Cramer, A. Granier, J. Ogee, and V. Allard (2007), Reduction of ecosystem productivity and respiration during the European summer 2003 climate anomaly: A joint flux tower, remote sensing and modelling analysis, *Glob. Chang. Biol.*, *13*(3), 634–651.
- Reichstein, M., M. Bahn, P. Ciais, D. Frank, M. D. Mahecha, S. I. Seneviratne, J. Zscheischler, C. Beer, N. Buchmann, and D. C. Frank (2013), Climate extremes and the carbon cycle, *Nature*, *500*(7462), 287–295.
- Sala, O., L. Gherardi, and D. C. Peters (2015), Enhanced precipitation variability effects on water losses and ecosystem functioning: Differential response of arid and mesic regions, *Clim. Chang.*, *131*(2), 213–227.
- Schar, C., P. L. Vidale, D. Luthi, C. Frei, C. Haberli, M. A. Liniger, and C. Appenzeller (2004), The role of increasing temperature variability in European summer heatwaves, *Nature*, *427*(6972), 332–336.
- van der Schrier, G., K. R. Briffa, T. J. Osborn, and E. R. Cook (2006), Summer moisture availability across North America, *J. Geophys. Res.*, *111*, D11102, doi:10.1029/2005JD006745.
- Schrier, G., J. Barichivich, K. Briffa, and P. Jones (2013), A scPDSI-based global data set of dry and wet spells for 1901–2009, *J. Geophys. Res. Atmos.*, *118*, 4025–4048, doi:10.1002/jgrd.50355.
- Screen, J. A. (2014), Arctic amplification decreases temperature variance in northern mid-to high-latitudes, *Nat. Clim. Chang.*, *4*(7), 577–582.
- Sheffield, J., E. F. Wood, and M. L. Roderick (2012), Little change in global drought over the past 60 years, *Nature*, *491*(7424), 435–438.
- Sippel, S., J. Zscheischler, M. Heimann, F. E. L. Otto, J. Peters, and M. D. Mahecha (2015), Quantifying changes in climate variability and extremes: Pitfalls and their overcoming, *Geophys. Res. Lett.*, *42*, 9990–9998, doi:10.1002/2015GL066307.
- Sitch, S., C. Huntingford, N. Gedney, P. Levy, M. Lomas, S. Piao, R. Betts, P. Ciais, P. Cox, and P. Friedlingstein (2008), Evaluation of the terrestrial carbon cycle, future plant geography and climate-carbon cycle feedbacks using five dynamic global vegetation models (DGVMs), *Glob. Chang. Biol.*, *14*(9), 2015–2039.
- Tucker, C. J., J. E. Pinzon, M. E. Brown, D. A. Slayback, E. W. Pak, R. Mahoney, E. F. Vermote, and N. El Saleous (2005), An extended AVHRR 8-km NDVI dataset compatible with MODIS and SPOT vegetation NDVI data, *Int. J. Remote Sens.*, *26*(20), 4485–4498.
- Wang, X., S. Piao, P. Ciais, J. Li, P. Friedlingstein, C. Koven, and A. Chen (2011), Spring temperature change and its implication in the change of vegetation growth in North America from 1982 to 2006, *Proc. Natl. Acad. Sci. U.S.A.*, *108*(4), 1240–1245.
- Watson, J. E. M., T. Iwamura, and N. Butt (2013), Mapping vulnerability and conservation adaptation strategies under climate change, *Nat. Clim. Chang.*, *3*(11), 989–994.
- Wu, X., H. Liu, Y. Wang, and M. Deng (2013), Prolonged limitation of tree growth due to warmer spring in semi-arid mountain forests of Tianshan, northwest China, *Environ. Res. Lett.*, *8*, 024016, doi:10.1088/1748-9326/8/2/024016.
- Wu, X., H. Liu, X. Li, E. Liang, P. S. Beck, and Y. Huang (2016), Seasonal divergence in the interannual responses of northern hemisphere vegetation activity to variations in diurnal climate, *Sci. Rep.*, *6*, doi:10.1038/srep19000.